ANNALS OF GEOPHYSICS, 67, 5, GC546, 2024; doi:10.4401/ag-9024
OPEN ACCESS

Physics of the Northern Annular Mode – Part 2: connection to meridional vorticity transfer

Aarnout J. van Delden[*,1]

(1) Institute for Marine and Atmospheric Research Utrecht (IMAU), Physics Department Utrecht University, Utrecht, the Netherlands

Article history: received October 13, 2023; accepted April 09, 2024

Abstract

A new perspective on the nature and cause of the Northern Annular Mode (NAM) is offered, by adopting isentropic coordinates, making use of the impermeability to vorticity fluxes of isentropic surfaces, and by avoiding the quasi-geostrophic approximation.
The NAM is identified with the zonal-mean circumpolar flow, also called the "primary circulation". The positive (negative) NAM-phase is characterized by a weaker (more intense) than average zonal-mean subtropical jet and also a more poleward (equatorward) than average position of the maximum zonal-mean surface westerlies. The negative NAM-phase is maintained by an intense residual circulation of mass, as explained in part 1 of this paper. The positive NAM-phase is maintained by up-gradient, therefore self-perpetuating, poleward eddy vorticity fluxes in the middle latitudes, which intensify the primary circulation in middle latitudes, while driving it out of gradient wind balance. As a response to the imbalance of the primary circulation, a zonal-mean meridional overturning circulation, or "secondary circulation", is generated in the middle latitudes. Vorticity fluxes due to the secondary circulation oppose eddy vorticity fluxes. On the monthly time-scale this opposition is nearly exact, implying a stationary state, were it not for the fact that the secondary circulation also transports mass, which, by opposing the eddy mass-flux, reduces the intensity of the residual (net) circulation of mass, and so prevents a transition to the negative NAM-phase.
A transition from one extreme NAM-phase to the opposite NAM-phase takes at least several days during which either the reservoir of mass (transition to negative NAM-phase) or the reservoir of vorticity (transition to positive NAM-phase) at high latitudes in the lowermost stratosphere and upper troposphere is replenished.

Keywords: Westerly wind; Balance; Eddies; Ferrel cell; Vorticity Flux; Impermeability

1. Introduction

This paper is the second part of two papers that address the physics of the Northern Annular Mode (NAM), defined in detail in part 1 (van Delden, 2024). A viewpoint in isentropic coordinates is taken. The rather restrictive quasi-geostrophic approximation is avoided. The structure of the general circulation atmosphere is divided into the following three interacting components: (1) a "primary" zonally symmetric (i.e. zonal-mean) circumpolar

circulation, (2) a "secondary" zonally symmetric meridional overturning circulation, consisting of the Hadley cells in the tropics and the Ferrel cells in the middle latitudes (Dima and Wallace, 2003), and (3) eddies and waves, or zonal asymmetries.

The primary circulation is defined by the zonal-mean zonal wind velocity, $[u]$ (symbols are defined in the appendix to this paper). The secondary circulation is defined by the zonal-mean meridional wind velocity, $[v]$. Both $[u]$ and $[v]$ depend on time, latitude and height. Height in this paper is measured in terms of potential temperature,

$$\theta = T\left(\frac{p_{ref}}{p}\right)^{\kappa}. \tag{1}$$

Meridional advective isentropic mass- and vorticity-fluxes, associated with eddies and with the secondary circulation, are referred to in short, respectively, as *eddy fluxes* and *mean fluxes*. The sum of eddy- and mean fluxes is referred to as the *net flux*, or the *residual flux*.

The NAM is identified with non-seasonal fluctuations in the primary circulation, specifically with coupled non-seasonal fluctuations of the strength of the zonal-mean Sub-Tropical Jet (STJ) and the latitude of the maximum zonal-mean surface westerlies, which is closely linked to the sea-level pressure distribution. The negative NAM-phase, for example, is characterized by (1) an intense zonal-mean STJ at the boundary between the tropical upper troposphere and the extratropical lowermost stratosphere, by (2) a very equatorward position of the most intense zonal-mean surface-westerlies, by (3) relatively weak sub-tropical high's in the Atlantic and Pacific Oceans and by (4) an intense and deep meridional residual circulation of mass. The aim is to identify feedback-loops in the interaction of the three components of the general circulation that can maintain the NAM in an extreme phase for an appreciable time. What physical processes, for example, are involved in the feedback loop that sustains an intense STJ and simultaneously sustains weak subtropical highs in the negative NAM-phase? This question is addressed in Part 1 of this paper.

In part 1 the persistence of the negative phase of the NAM is explained as being due to a self-sustaining feedback-loop between baroclinicity below the STJ and the net meridional isentropic mass-flux divergence just poleward of the STJ in the upper poleward branch of the residual circulation of mass. Mass-flux divergence is driven by eddies feeding on the available potential energy associated with baroclinicity, which, in turn, is itself sustained by the meridional mass-flux divergence.

The present paper (part 2) provides further details of the driving of the NAM and offers a physical explanation of the persistence of the positive phase of the NAM, which is characterized by a relatively weak zonal-mean STJ, a relatively weak and shallow zonal-mean baroclinic zone, a more poleward position of the most intense zonal-mean surface westerlies and a weak and shallow meridional circulation of mass.

Important findings and conclusions of part 1 of this paper are the following.

1) The primary circulation, i.e. the zonal mean circumpolar flow, is in very close thermal wind balance. This means that the structure of the primary circulation, such as the strength of the STJ, depends on the zonal-mean potential vorticity (PV) distribution, in accord with a zonal-mean potential vorticity (PV) – inversion equation, which is an expression of zonal-mean thermal wind balance in terms of zonal-mean potential vorticity.
2) A feature of the zonal-mean potential vorticity distribution that stands out is the positive PV-anomaly centered over the pole, approximately between the dynamical tropopause and the 370 K isentrope. This PV-anomaly, which is manifest principally as a negative isentropic density anomaly, defines the lowermost stratosphere. The STJ is found at the equatorward edge of this PV-anomaly, in accordance with the solution of the zonal-mean PV-inversion equation.
3) The positive PV-anomaly, defining the lowermost stratosphere, derives its identity from the fact that this layer has lost a large fraction of its mass, by cross-isentropic downwelling due to radiative flux divergence, to a dome of potentially cold air residing over the high latitude Northern Hemisphere.
4) The intensity of the residual meridional mass-flux fluctuates between intense phases and weak phases. The intense phase may consist of a series of mass-flux pulses each lasting at least 5 days or much longer. The weak phase consists of shorter and weaker mass-flux pulses.
5) The intense and weak phases of the extratropical meridional circulation of mass are manifest at the earth's surface as a seesaw in pressure between the subtropical belt of high pressure and the zonal belt of relatively low pressure over the Polar Cap. The negative (positive) NAM phase is associated with a weakening/reversal (strengthening) of the zonal mean sea-level pressure gradient between subtropics and higher latitudes.

Part 1 of this paper does not answer the question how exactly the secondary circulation and eddies separately drive the primary circulation and associated zonal mean distribution of mass and vorticity. This question is the subject of part 2. Section 2 of part 2 introduces the phenomenon of *planetary wave breaking* and the associated isentropic *potential vorticity mixing*. Section 3 explains the idea of vorticity as the concentration of a substance, called *Potential Vorticity Substance* (PVS), and derives a PVS-flux equation. In section 4 the contributions to the advective PVS-flux due to, respectively, the secondary circulation and eddies are identified. From reanalysis data it is shown that advective PVS-fluxes dominate the PVS-budget, but that this budget differs strongly in the respective extreme NAM-phases. Section 5 offers an explanation for the persistence of the positive NAM-phase. Section 6 discusses the connection between the meridional eddy PVS-flux and the meridional residual mass-flux. Section 7 investigates a particular NAM-phase transition and demonstrates that the positive NAM phase is characterized by short planetary waves in middle latitudes, which propagate eastward relatively quickly, while slow eastward propagating long planetary waves characterize the negative NAM-phase. Section 8 concludes this paper.

2. Isentropic potential vorticity mixing due to breaking planetary waves

Figure 1 shows the evolution of the potential vorticity field and the zonal wind velocity on the 350 K isentropic surface in the Northern Hemisphere at 24-hour intervals, between 00 UTC on 13 December 2006 and 00 UTC on 15 December 2006. Potential vorticity (PV) in isentropic coordinates (Z_θ) is defined as

$$Z_\theta = \frac{\zeta_a}{\sigma}, \tag{2}$$

where absolute vorticity is the sum of relative vorticity (ζ) planetary vorticity (f),

$$\zeta_a \equiv \zeta + f\,, \tag{3}$$

and isentropic density,

$$\sigma = -\frac{1}{g}\frac{\partial p}{\partial \theta}. \tag{4}$$

Vorticity and isentropic density are core variables in the understanding of the dynamics of the atmosphere in isentropic coordinates, i.e. with potential temperature, θ, as the vertical coordinate. Other variables are defined in the appendix to this paper.

The following two regions of approximately uniform potential vorticity (PV) can be distinguished at $\theta = 350$ K in Fig. 1. A region shaded in red in the tropics is characterized by PV-values less than 1 PVU, while the region shaded in blue in the extra-tropics is characterized by much higher PV-values (5-8 PVU). By definition, the first region lies in the troposphere, while the second region lies in the lowermost stratosphere. The relatively narrow transition zone in between encompasses the isentropic tropopause, which is usually identified by the 2 PVU isopleth of PV (Ambaum, 1997) (1 PVU, or Potential Vorticity Unit, is equivalent to 10^{-6} $s^{-1}kg^{-1}Km^2$).

In adiabatic conditions an air-parcel remains on an isentropic surface and conserves its potential vorticity (PV). Adiabatic conditions indeed seem to prevail over the period of two days on the 350 K isentropic surface in December 2006, shown in Fig. 1. We observe poleward intrusions of tropical (tropospheric) low-PV air and equatorward intrusions of extra-tropical (stratospheric) high-PV air. A tropical air mass can be identified at about 30°W (i.e. over the Eastern Atlantic Ocean), as it intrudes into the middle latitudes. This intrusion represents the crest of a planetary wave, which appears to "break", like a breaking ocean wave. The intruded tropical low-PV air mass seems to return to the tropics following a clockwise (anticyclonic) trajectory, as if a "restoring force" is driving this low-PV air mass back to its "equilibrium position". In the case of ocean waves, gravity is responsible for the restoring force that drives the water parcels back to their equilibrium position. In Fig. 1, it appears as if an analogous "restoring force"

is driving the tropical air back to the tropics. What is the origin of this mysterious "elasticity"? An understanding of the source of this so-called "elasticity" comes in section 4.

Planetary wave breaking may appear as cyclonic wave breaking or as anticyclonic wave breaking (Bennedict et al., 2004). Anticyclonic planetary wave breaking, in which low-PV tropical air moves polewards and is deflected eastward, thus rotating anticyclonically, is observed in Fig. 1 between the longitudes of 30°W and 30°E.

The crests of breaking planetary waves are associated with "rapids" in the subtropical jet stream, called "jet-streaks", which move to relatively high latitudes (about 60°N), preferably over the North-Eastern Atlantic or Pacific Oceans, where these jet-streaks are the seat of cyclogenesis. One such jet-streak", with a length of several thousands of kilometers, is observed in Fig. 1 moving from the Atlantic Ocean to Scandinavia.

Planetary waves and cyclones are excited and grow in amplitude due (1) baroclinic instability, due to (2) thermal (inertia) contrasts between continents and oceans, due to (3) the interaction of the mean zonal flow with the inhomogeneous surface of the earth, and due to (4) tropical deep convection, especially over South East Asia. Enhanced wave activity in the form of breaking waves, forming closed eddies (cyclones and anticyclones), is frequently observed in three preferred regions: (1) over the Eastern Pacific and adjacent Western North America, (2) over the Eastern Atlantic and adjacent Europe, and (3) over Japan.

Isentropic potential vorticity (PV)-mixing due to planetary wave breaking is reflected in the time-mean isentropic PV-distribution as a reduction of the isentropic meridional gradient of potential vorticity within the mixing-zone (see Fig. 5 of McIntyre, 1982). Figure 2 shows the 1 PVU- and 7 PVU-isopleths of PV at $\theta = 350$ K in January 2007 (a)

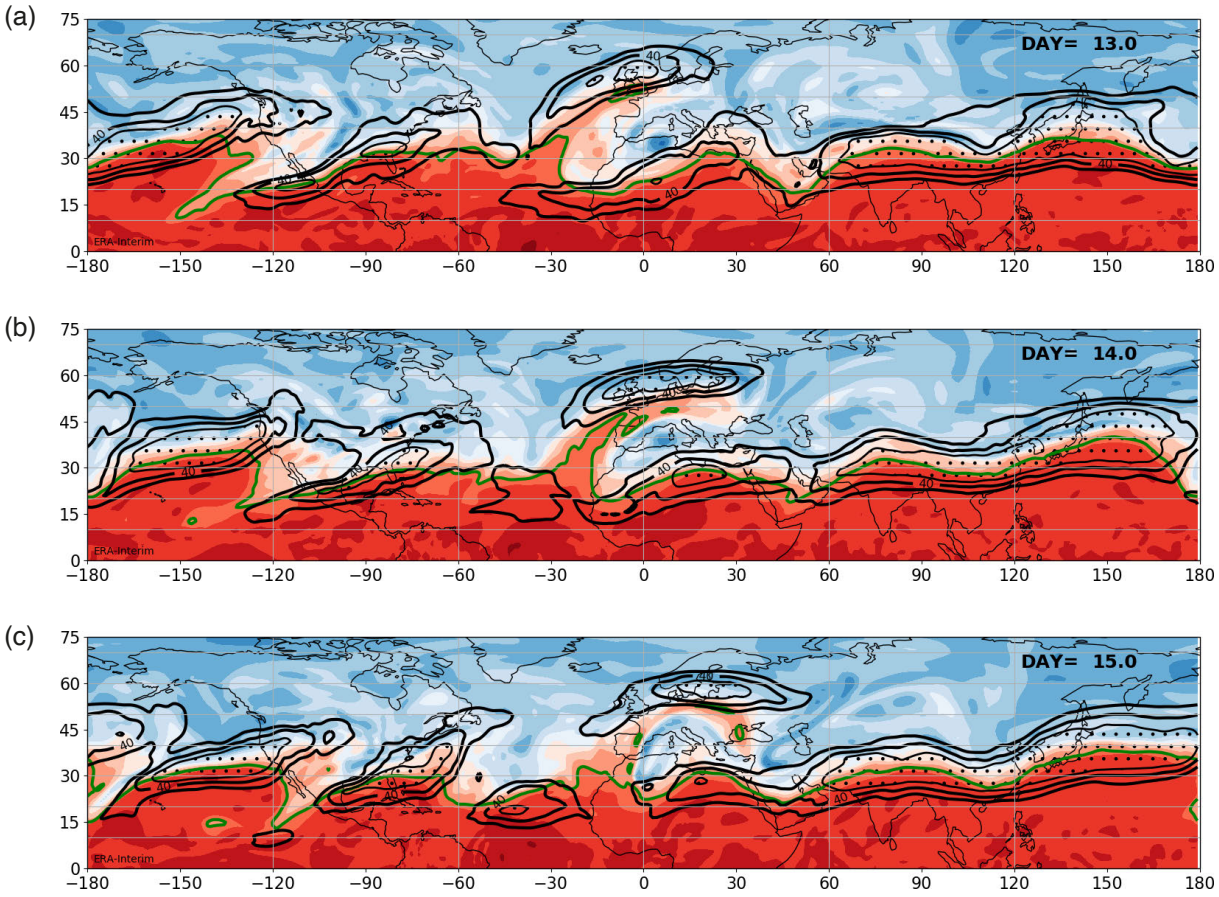

Figure 1. Illustrating planetary wave breaking. Potential vorticity (Z_θ) and zonal wind velocity (u) on the 350 K isentropic surface, as a function of latitude (°N) (ordinate) and longitude (°E) (abscissa) at 00 UTC, 13 December 2006 (a), 14 December 2006 (b) and 15 December 2006 (c). Red shading corresponds to $Z_\theta < 5$ PVU. Blue shading corresponds to $Z_\theta > 5$ PVU. The green contour is defined as the isentropic dynamical tropopause ($Z_\theta = 2$ PVU). Black contours of u are drawn for 30, 40 and 50 m/s. In dotted regions, $u > 50$ m/s. An ideal example of (anti-cyclonic) planetary wave breaking is observed between the longitudes of 30°W and 30°E, affecting potential vorticity and zonal wind between the latitudes, 30°N and 60°N. Based on the ERA-Interim reanalysis (Dee et al., 2011).

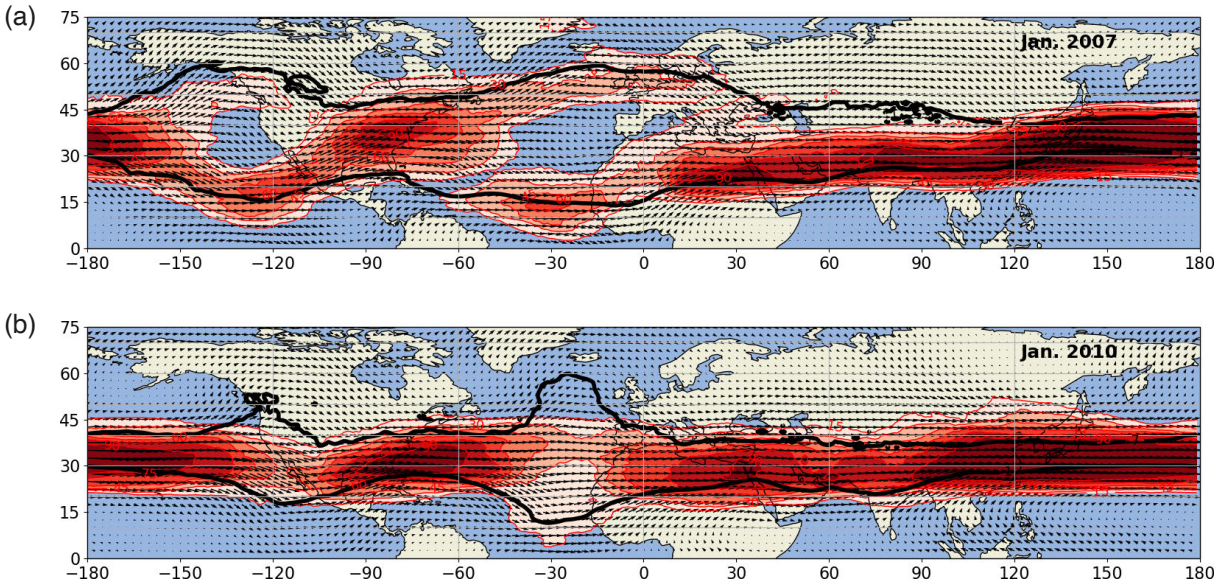

Figure 2. Fraction of time that the zonal wind velocity, u, exceeds 35 m s^{-1} (red contours and red shading) at $\theta = 350$ K in January 2007 (a) and in January 2010 (b) as a function of latitude (°N) (ordinate) and longitude (°E) (abscissa). Contour-interval is 15%, starting at 15 %. Also shown are monthly average wind vectors at $\theta = 350$ K and the 1 PVU- and 7 PVU-isopleths of monthly average potential vorticity at $\theta = 350$ K. Based on the ERA-Interim reanalysis (Dee et al., 2011).

and in January 2010 (b). A large meridional distance between these PV-isopleths in January 2007 indicates PV mixing by planetary wave breaking occurring over a larger range of latitudes. Wave breaking was most frequently of the anti-cyclonic type in January 2007, occurring preferably in the North-East Pacific and Western Canada and over the North-East Atlantic and Europe. The frequent occurrence of jet-streaks on the crests of the anti-cyclonically breaking waves in January 2007 is revealed in Fig. 2a. Two high latitude maxima in the frequency of the occurrence of high zonal wind speeds, next to the continuous frequency-maximum at lower (sub-tropical) latitudes, are observed in the longitude ranges, −150° to −120° and −40° to + 30°. Although there is some indication of wave breaking and attendant PV-mixing in January 2010 (Fig. 2b), this is hardly associated with anticyclonic wave breaking, given the relative absence of high zonal wind velocities at 350 K at high latitudes in January 2010.

3. Potential vorticity substance flux

The intensity of meridional PV-mixing due to planetary wave breaking is usually measured in terms of a meridional eddy-flux of potential vorticity. This, indeed, is the approach commonly adopted in quasi-geostrophic theory in pressure coordinates. For reasons given in part 1 of this paper (van Delden, 2024), we avoid the quasi-geostrophic approximation and adopt isentropic coordinates. One of the most remarkable and useful properties of potential vorticity in isentropic coordinates is that it can be regarded as the mixing ratio of a substance, called "potential vorticity substance", abbreviated as "PVS", which cannot be transferred across isentropic surfaces. This is trivial in adiabatic conditions, for which

$$\frac{d\theta}{dt} = 0, \tag{5}$$

but this is true also for hydrostatic flow in the atmosphere under all conditions. Haynes and McIntyre (1990) demonstrated that the vorticity equation in isentropic coordinates can be written as

$$\frac{\partial \zeta_a}{\partial t} = -\vec{\nabla}_\theta \cdot \vec{J}, \tag{6}$$

where

$$\vec{\nabla}_\theta \equiv \left(\left(\frac{\partial}{\partial x}\right)_\theta, \left(\frac{\partial}{\partial y}\right)_\theta, \frac{\partial}{\partial \theta}\right) \tag{7}$$

and

$$\vec{J} \equiv \left(u\zeta_a + \frac{d\theta}{dt}\frac{\partial v}{\partial \theta} - F_y, v\zeta_a - \frac{d\theta}{dt}\frac{\partial u}{\partial \theta} + F_x, 0\right) \tag{8}$$

represents the flux of PVS. In Eq. (8), F_x and F_y are the x-component and y-component, respectively, of an arbitrary frictional force per unit mass. Note that the cross-isentropic component of the PVS-flux vector, $\vec{J}$, is equal to zero. This implies that isentropic surfaces are impermeable to PVS under all circumstances. This statement is known as the "Impermeability theorem for potential vorticity substance".

The adiabatic advective component of the PVS-flux vector is

$$\vec{J} \equiv (u\zeta_a, v\zeta_a, 0). \tag{9}$$

If potential vorticity can be regarded as the mixing ratio of PVS, absolute vorticity can be interpreted as the *concentration* of PVS, analogous to isentropic density, or concentration of mass, σ, which obeys the following conservation equation

$$\frac{\partial \sigma}{\partial t} = -\vec{\nabla} \cdot \vec{I}, \tag{10}$$

where the mass-flux vector is

$$\vec{I} \equiv \left(u\sigma, v\sigma, \frac{d\theta}{dt}\sigma\right). \tag{11}$$

Note that, while the PVS-flux, $\vec{J}$, has no component across an isentropic surface, the mass-flux, $\vec{I}$, has a cross-isentropic component when conditions are non-adiabatic.

The analogy of PVS with a substance is a valuable way of interpreting the dynamics of the atmosphere, but we should be aware of the following two caveats of this interpretation; (1) the mixing ratio of PVS is not a dimensionless quantity, as is the mixing ratio of real chemical substance, such as water vapor, and (2) unlike the amount of a real chemical substance, the "amount of PVS" may be negative.

4. The intensity of the primary circulation is determined by advective vorticity-fluxes

This section derives an equation linking the local time rate of change of $[u]$, to the zonal-mean meridional flux of vorticity. The starting point of this derivation is the x-component of the momentum equation for frictionless hydrostatic flow in isentropic coordinates (Dutton, 1976):

$$\frac{\partial u}{\partial t} + u\left(\frac{\partial u}{\partial x}\right)_\theta + v\left(\frac{\partial u}{\partial y}\right)_\theta + \frac{d\theta}{dt}\frac{\partial u}{\partial \theta} = -\left(\frac{\partial \Psi}{\partial x}\right)_\theta + fv + \frac{u\,v\tan\phi}{a}. \tag{12}$$

Here, Ψ is the isentropic streamfunction (see the list of symbols). Neglecting the curvature term (last term on r.h.s. of Eq. 12), which is important only at high latitudes ($> 75°$), and for high wind speeds ($> 100\ \mathrm{m\,s^{-1}}$), and assuming

adiabatic conditions, Eq. (12) becomes

$$\frac{\partial u}{\partial t} = -\frac{1}{2}\left(\frac{\partial(u^2)}{\partial x}\right)_\theta - \frac{1}{2}\left(\frac{\partial(v^2)}{\partial x}\right)_\theta + v\zeta - \left(\frac{\partial \Psi}{\partial x}\right)_\theta + fv \tag{13}$$

where the relative vorticity is (again neglecting the effect of earth's curvature),

$$\zeta = \left(\frac{\partial v}{\partial x}\right)_\theta - \left(\frac{\partial u}{\partial y}\right)_\theta. \tag{14}$$

Taking the zonal mean, indicated by square brackets, of Eq. (13) yields

$$\frac{\partial [u]}{\partial t} = [v\zeta] + f[v] = [v\zeta_a]. \tag{15}$$

This remarkably simple equation states that the zonal-mean advective PVS-flux determines the time-rate of change of the zonal-mean zonal velocity in adiabatic conditions. Reanalysis data, such as the ERA-Interim reanalysis of wind velocity and vorticity, given at 6-hour intervals (0, 6, 12 and 18 UTC), can be used to evaluate both sides of Eq. (15). Let us choose an interval of 1 day. This interval is equivalent to four time-steps in the ERA-Interim reanalysis. Therefore, the change of $[u]$ over 1 day is

$$\Delta[u] \approx [u]_{n+2} - [u]_{n-2}, \tag{16}$$

where n is the index of time. The daily mean zonal-mean PVS-flux, $\bar{F}$, is evaluated from

$$\bar{F} = (F_{n-2} + 2F_{n-1} + 2F_n + 2F_{n+1} + F_{n+2})/8, \tag{17}$$

where $F_n = [v\zeta_a]_n$.

Figure 3a demonstrates that $\bar{F}$ and $\Delta[u]$ are on average almost equal in January 2007, implying that intensifications ($\Delta[u] > 0$) or weakenings ($\Delta[u] < 0$) of the zonal-mean eastward wind over one-day intervals are dominantly determined by the advective PVS-flux. In other words, diabatic and frictional effects are quite negligible. Three reasons can be given for the slight difference (on average!) between $\bar{F}$ and $\Delta[u]$: (1) a small diabatic contribution to the PVS-flux (Eq. 8), (2) the neglect of the curvature term in Eq. (12), and (3) a numerical error because the PVS-flux is known only at discrete timings.

Following the method introduced in section 3 of van Delden (2024), we write the variables, v and ζ, as a sum of a zonal mean, indicated by square brackets, and a deviation from the zonal mean, indicated by an asterisk, as $v \equiv [v] + v^*$ and $\zeta \equiv [\zeta] + \zeta^*$. With this, Eq. (15) becomes

$$\frac{\partial [u]}{\partial t} = [v]([\zeta] + f) + [v^*\zeta^*]. \tag{18}$$

Assuming adiabatic (isentropic) and frictionless conditions, Eq. (18) is exact. The advective PVS-flux (r.h.s. of Eq. 18) is split into the following two components: (1) the meridional vorticity-flux due to the zonal-mean meridional overturning secondary circulation (first term on the r.h.s. of Eq. 18), and (2) the meridional vorticity-flux due to eddies (second term on the r.h.s. of Eq. 18). Component one is referred to in short as the "*mean PVS-flux*".

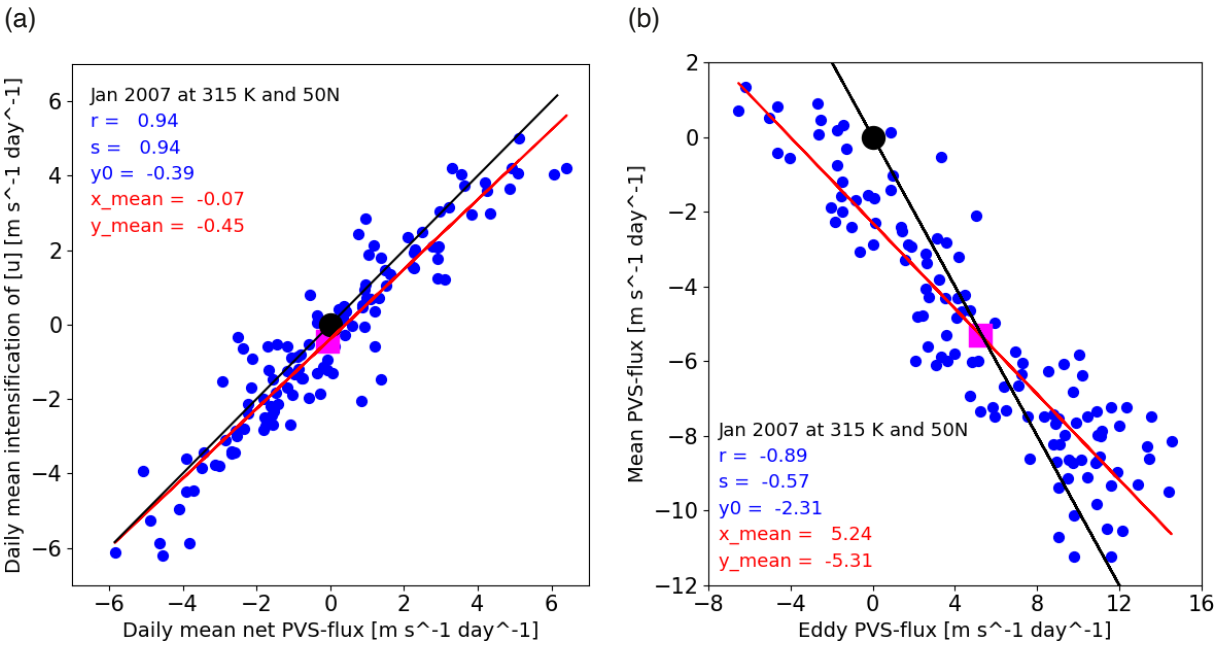

Figure 3. Showing that the change of $[u]$ over one-day intervals is explained very well by Eq. (15). (a) Change of the eastward zonal-mean zonal wind per day (Eq. 16), at 50°N and $\theta = 315$ K, for all overlapping one-day intervals in January 2007 as a function of the net advective isentropic vorticity (PVS) flux (r.h.s. of Eq. 15), averaged over the corresponding one-day interval. (b) The *mean* PVS-flux as a function of the *eddy* PVS-flux at 50°N and $\theta = 315$ K for all overlapping one-day intervals in January 2007. The red straight line in both panels represents the best linear fit. The associated correlation coefficient, r, and slope, s, are indicated in the plot. The magenta square represents the monthly average. The black straight line in both panels is the "one-to-one" line with slope, $s = 1$, intersecting the origin (black dot). The red straight line converges towards the black line with increasing averaging time, as is seen by comparison with Fig. 4. Based on the ERA-Interim reanalysis (Dee et al., 2011).

Component two is referred to in short as the "*eddy PVS-flux*". The sum of *mean* and *eddy* PVS-fluxes is referred as the *net* (or *residual*) PVS-flux.

Figure 3b shows a scatter plot of the daily mean *mean* PVS-flux against the daily mean *eddy* PVS-flux at 50°N and 315 K. *Eddy* PVS-fluxes are mostly positive, while *mean* PVS-fluxes are mostly negative. This means that eddies usually *intensify* the zonal-mean eastward wind over one-day intervals. The eddy PVS-flux is usually opposed by the mean PVS-flux, but it seems that the mean PVS-flux cannot compensate the eddy PVS-flux if the eddy PVS-flux exceeds about 5 $\mathrm{m\,s^{-1}\ day^{-1}}$. Indeed, a near balance between mean PVS-flux and eddy PVS-flux is usually not observed over one-day intervals. Taking the monthly average of all one-day periods reveals, however, that this near balance does exist on a monthly time-scale. In other words, the *mean* meridional PVS-flux is approximately equal and opposite to the *eddy* meridional PVS-flux according to,

$$\int_0^\tau [v]([\zeta] + f)dt = -\int_0^\tau [v^*\zeta^*]dt, \tag{19}$$

if $\tau = 1$ month. In January 2007, at 50°N and 315 K, the left-hand side of Eq. (19) is $-5.31\ \mathrm{m\,s^{-1}}$ per day while right-hand side of Eq. (19) is $+5.24\ \mathrm{m\,s^{-1}}$ per day (Fig. 3). In other words, on a monthly time-scale, eddies intensify the primary circulation, while the secondary circulation opposes this eddy-effect almost exactly. Figure 4 demonstrates that this is true to an impressively high degree at 50°N and 315 K for all months of January between 1979 and 2018. Quantitatively, however, the balance between eddy- and mean fluxes differs appreciably in different years, with January 2007 (red dot) and January 2010 (blue dot) as extremes. The distribution of January-mean eddy PVS-fluxes is skewed: above average eddy PVS-fluxes occur more frequently than below average eddy PVS-fluxes, but below average eddy PVS-fluxes are more extreme.

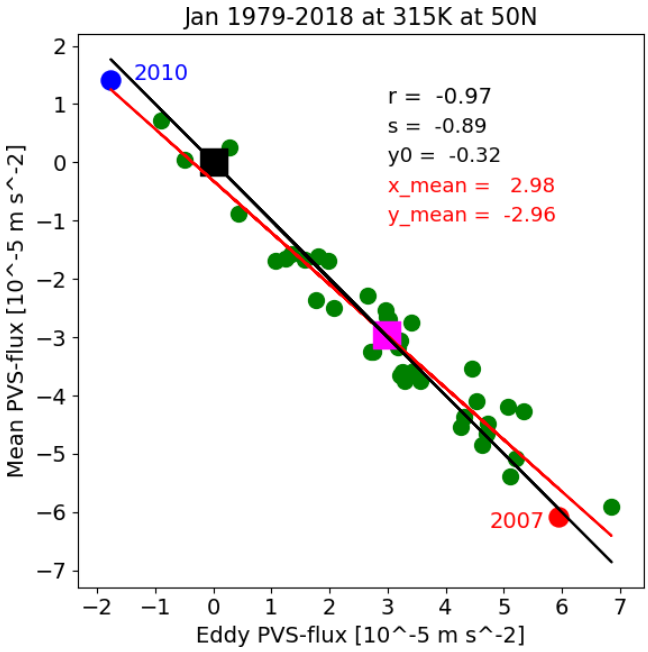

Figure 4. Showing that eddy- and mean PVS-fluxes oppose each other almost exactly on the monthly time-scale. January-average *mean* isentropic PVS-flux, $[v]([\zeta]+f)$, as a function of the January-average *eddy* isentropic PVS-flux, $[v^*\zeta^*]$, at 315 K and 50°N, in the years 1979-2018. The black straight line has slope, $s=1$, and intersects the origin (black square). The red straight line represents the best linear fit to the 40 points (correlation coefficient is −0.97). The slope of this line is $s=-0.89$ and crosses the y-axis at $y=-0.32\times10^{-5}\,\mathrm{m\,s^{-2}}$. The magenta square represents the ensemble average value for all 40 months of January. The ensemble average eddy PVS-flux ($+2.98\times10^{-5}\,\mathrm{m\,s^{-2}}$) is in close balance with the ensemble average mean PVS-flux ($-2.96\times10^{-5}\,\mathrm{m\,s^{-2}}$). The blue dot is for January 2010 (extreme negative NAM phase); the red dot is for January 2007 (extreme positive NAM phase). Based on the ERA-Interim reanalysis (Dee et al., 2011).

By examining the two terms, which make up the net advective PVS-flux (r.h.s. of Eq. 18), in a large range of latitudes and levels in the Northern Hemisphere, we find that eddies intensify the zonal-mean eastward flow in a broad range of middle latitudes in the Middleworld (above 300 K) (left panels of Fig. 5). The equatorward edge of this range of latitudes coincides approximately with the latitude of the STJ at 30°N. The poleward edge of the region of poleward eddy PVS-fluxes in middle latitudes, which presumably reflects the poleward edge of anticyclonically breaking planetary waves (Fig. 1 and Fig. 2), is found at about 60°N in January 2007 and at about 50°N in January 2010.

Meridional eddy PVS-fluxes in middle latitudes mostly intensify the primary circulation, thereby driving the atmosphere away from zonal-mean gradient wind balance and creating super-gradient zonal-mean zonal winds. The associated imbalance of forces in the meridional direction generates a secondary zonally symmetric meridional overturning circulation, which is referred to also as the "Ferrel cell". Eliassen (1951) and Kuo (1956) demonstrated theoretically that the Ferrel cell acts to restore gradient wind balance of the primary circulation. In January 2007 the monthly average eddy PVS-flux peaks at just over $8\times10^{-5}\,\mathrm{m\,s^{-2}}$ at 50°N and 330 K (250 hPa), which would intensify the zonal-mean eastward flow by about $7\,\mathrm{m\,s^{-1}}$ per day if it were not countered almost exactly by the mean PVS-flux (right panels of Fig. 5). The monthly average eddy PVS-flux in January 2010 peaks at a similar value, but just south of 40°N, and somewhat higher at 350 K (200 hPa).

The panels on the right of Fig. 5 demonstrate that the mean PVS-flux counteracts the eddy PVS-flux almost exactly on a monthly time-scale at most levels and latitudes. This implies that the rates of intensification of the zonal-mean eastward wind over monthly intervals are very small relative to the rates of intensification of the zonal-mean eastward wind over daily intervals (Fig. 3). The secondary circulation, which is also known as the "ageostrophic response" to eddy-driving and exists in order to maintain the zonal-mean zonal wind velocity in approximate zonal-mean gradient wind balance in the face of "eddy-driving", is able to achieve this goal much better on the monthly time-scale than on the daily time-scale. The close balance between the eddy PVS-flux (driving the zonal mean state away from balance) and the mean PVS-flux (driving the zonal mean state back into balance) is a

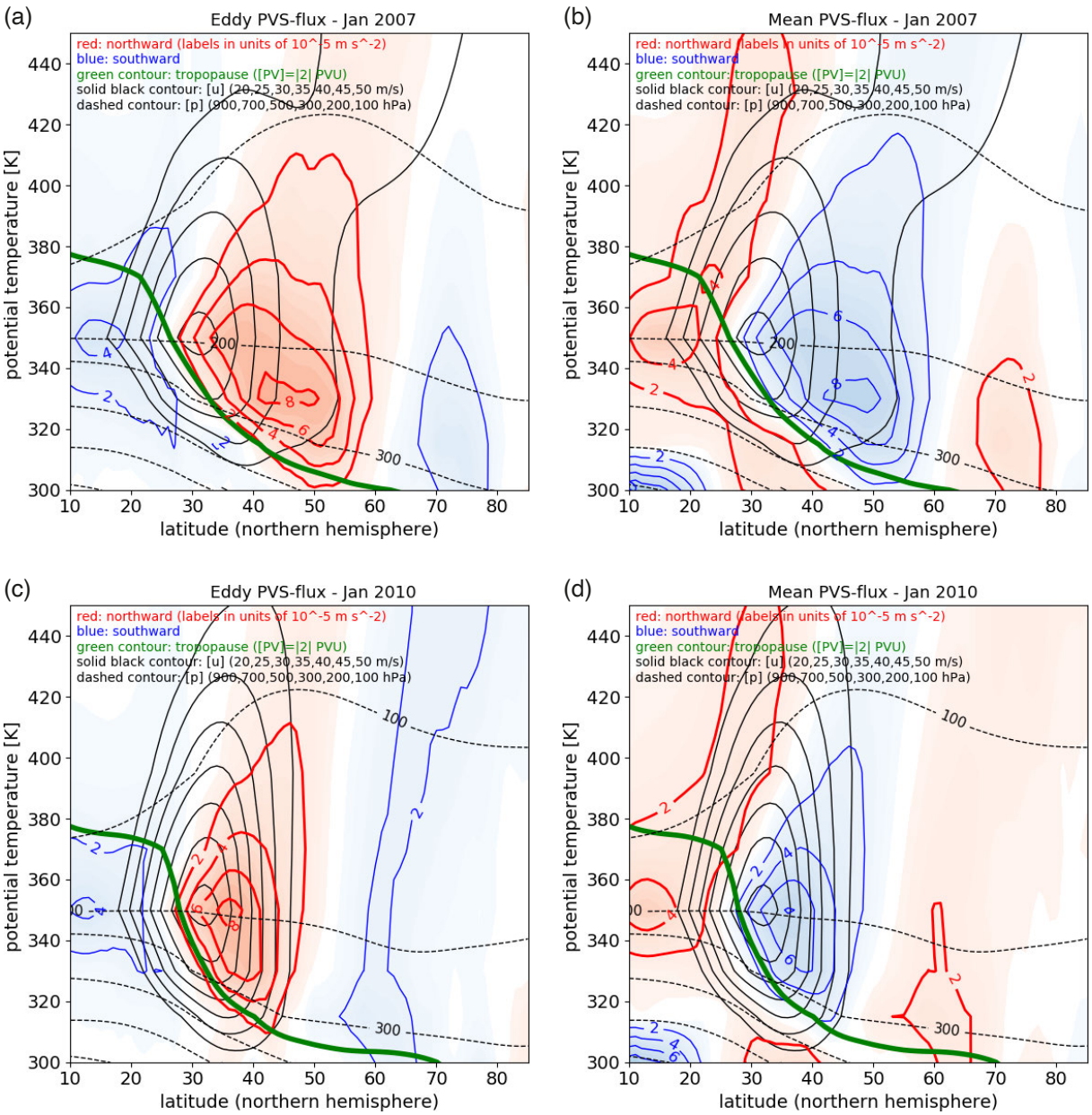

Figure 5. January-mean, zonal-mean isentropic PVS-flux as a function of latitude and potential temperature in 2007 (upper panels) and in 2010 (lower panels). Left panels: eddy PVS-flux, $[v^*\zeta^*]$. Right panels: mean PVS-flux, $[v]([\zeta]+f)$. Red shading corresponds to northward (positive) PVS-fluxes. Blue shading corresponds to southward (negative) PVS-fluxes. Labels are in units of 10^{-5} m s^{-2}. Also shown are the monthly average, zonal-mean pressure (dashed contours) (labeled in hPa), the 2 PVU dynamical tropopause (green solid contour) and the zonal-mean zonal wind velocity (black solid contours, drawn at 5 m s^{-1} intervals, starting at 20 m s^{-1}). Based on the ERA-Interim reanalysis (Dee et al., 2011).

manifestation of "geostrophic turbulence", a term coined by Jules Charney (1971). The ageostrophic response is an important reason for the apparent "elasticity" of breaking planetary waves (Fig. 1), alluded to in section 2.

5. Up-gradient eddy PVS-fluxes drive the NAM into its positive phase

It is an every-day observation that mixing by turbulent eddies of a substance, which is initially concentrated non-homogeneously, ends when the substance is concentrated homogeneously. This is because turbulent fluxes act only in the presence of a concentration gradient. This observation translates into the hypothesis that the turbulent

flux of a materially conserved quantity is directed down the mean spatial gradient of its concentration. More mathematically, this hypothesis states that the turbulent flux, $\vec{J}$, of a materially conserved quantity is proportional to the spatial gradient of the concentration, φ, of this quantity as

$$\vec{J} = -D\vec{\nabla}\varphi. \tag{20}$$

Here, D is a *positive* diffusion coefficient, i.e. the flux is proportional to the negative of the concentration gradient. This is an expression of Fick's law. A down-gradient turbulent flux of a substance acts to reduce the gradient of the concentration of this substance and so also to reduce the flux of this substance. This process represents a negative feedback loop.

Do eddy PVS-fluxes obey Fick's law? Since vorticity can be interpreted as the concentration of substance called Potential Vorticity Substance (PVS), we can check the applicability of Fick's law to monthly average eddy PVS-fluxes. Figure 6 shows a scatter plot of the January-mean meridional eddy PVS-flux at 330 K, between the latitudes, 45°N and 55°N, as a function of the corresponding January-mean meridional PVS-gradient between 45°N and 55°N. The linear regression shown in Fig. 6 (the red line) suggests that there is a linear relation between the meridional flux of PVS by large-scale atmospheric eddies and the meridional gradient of PVS. The correlation coefficient is 0.78, with a standard error of 0.06. So, indeed, eddy PVS-fluxes in middle latitudes obey Fick's law approximately. But note that both the PVS-flux and the PVS-concentration gradient are positive! Therefore, Fick's law applies here only if the associated diffusion coefficient, D, is negative. The poleward eddy PVS-flux acts to increase the positive meridional

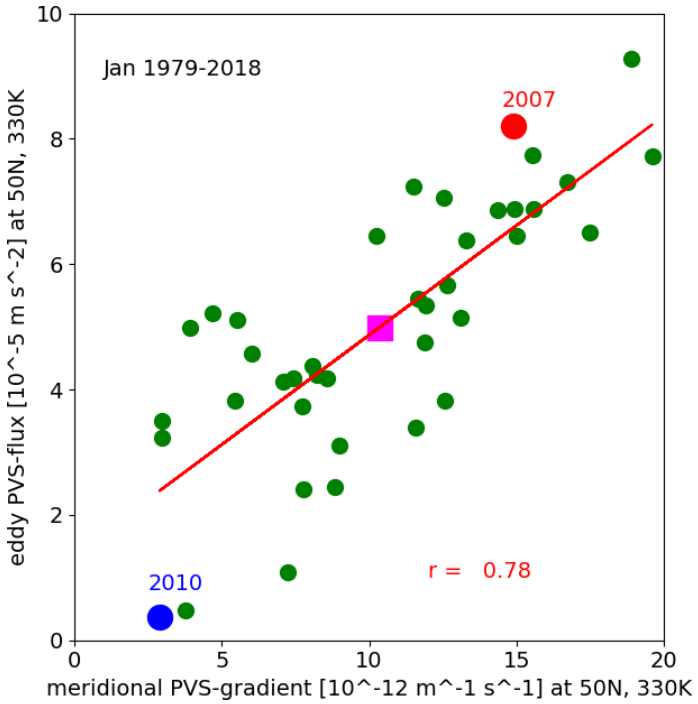

Figure 6. Demonstrating that the meridional eddy PVS-flux at 50°N and 330 K is directed up the local meridional PVS-gradient, which is principally determined by the positive value of *planetary* vorticity at 50°N, $\beta = 14.7 \times 10^{-12}$ m^{-1}s^{-1}. Dots represent the January-mean, zonal-mean meridional eddy PVS-flux at $\theta = 330$ K at 50°N in the years 1979-2019, as a function of the zonal-mean meridional gradient of the January-mean absolute vorticity. The meridional gradient is calculated by taking the difference of the absolute vorticity at 45°N and at 55°N and dividing by the distance between these two parallels. The red dot represents January 2007 (extreme positive NAM-index). The blue dot represents January 2010 (extreme negative NAM-index). The magenta square represents January ensemble average for the years 1979-2018. The correlation coefficient, r, of the linear fit (the red line) to the 40 data points is 0.78 with a standard error of 0.06. Based on the ERA-Interim reanalysis (Dee et al., 2011).

gradient of PVS, and hence also acts to further intensify the poleward eddy PVS-flux. Have we identified a positive feedback loop, which might explain the persistence of the extreme positive NAM phase? Victor Starr (1909-1976), who stood at the forefront of early studies of large-scale atmospheric transport phenomena, became so acutely aware of the possibility of such an unusual flux-gradient relationship that he felt obliged to write a book on this topic, entitled "*Negative Viscosity Phenomena*" (Starr, 1968). For a more recent paper on this topic, see Birner et al. (2013).

Why this unusual flux-gradient relationship? A clue to the answer to this question was given by Starr (1948), who suggested that the horizontal transfer of momentum is brought about by the large-scale troughs and ridges in the mid-troposphere, which are adapted to perform this function by their departure from a sinusoidal form. Converging westerly momentum transfer by eddies and poleward vorticity transfer by eddies are theoretical manifestations of an identical process (Kuo, 1951). Numerical simulations of baroclinic planetary wave life-cycles, by e.g. Thorncroft et al., (1993) and Balasubramanian and Garner, (1997), have shown that the trough and ridge lines in the horizontal plane of planetary waves in the middle latitudes of the Northern Hemisphere have the propensity to tilt forward from south-west to north-east, due to the positive meridional gradient of the planetary vorticity, $\beta = \mathrm{d}f/\mathrm{d}y > 0$ (the so-called "β–effect"). It must be added that convergence of the meridians may also play a role in promoting this forward tilt. A forward wave-tilt of planetary waves means that $[u^*v^*] > 0$, implying that westerly momentum in the Northern Hemisphere is transferred poleward and must converge at higher latitudes. Convergence of the eddy flux of westerly momentum and attendant intensification of the zonal-mean zonal wind is usually observed to occur between 50°N and 60°N (see Fig. 1 of Starr, 1948). A forward wave-tilt also promotes anticyclonic wave breaking, as in the case shown in Fig. 1.

The vorticity-flux-gradient relationship, shown in Fig. 6, suggests that we can generalize the conclusions of the above-mentioned numerical experiments to the meridional gradient of the *absolute* vorticity of the flow in the background of the planetary waves. At 50°N, the planetary vorticity-gradient, $\beta = 14.7 \times 10^{-12}\ \mathrm{m^{-1}s^{-1}}$. The monthly-mean meridional gradient of *absolute* vorticity between 45 and 55°N, at 330 K, is greater than planetary vorticity gradient in 9 out of 41 months of January between 1979 and 2019. Among these 9 months is January 2007, which is characterized by a very intense poleward eddy vorticity-flux and frequent anticyclonic wave breaking. On the other side of the spectrum is January 2010, which a characterized by a very weak, although still positive, monthly-mean meridional gradient of absolute vorticity between 45 and 55°N, a very weak monthly-mean poleward eddy vorticity-flux and less frequent anticyclonic wave breaking (Fig. 1).

6. Poleward eddy PVS-fluxes indirectly weaken the poleward mass-flux

Differences between the negative NAM-phase and the positive NAM-phase, in terms of the amplitudes of eddy PVS- and mass-fluxes, are most apparent in the latitude-band between 50°N and 60°N (Fig. 5). In the positive NAM-phase, the mean mass-flux, $[v][\sigma]$, in this latitude band, acts to oppose the mostly poleward eddy mass-flux, thereby weakening the net poleward mass-flux, which prevents a transition to the negative NAM-phase.

On a monthly time-scale, both the mean PVS-flux, $[v]([\zeta] + f)$, and the mean mass-flux, $[v][\sigma]$, are strongly anti-correlated with the eddy PVS-flux, $[v^*\zeta^*]$, as can be seen in, respectively, Fig. 4 and Fig. 7. This effect is important especially between 50°N and 60°N, because of the large year-to-year variability of the eddy PVS-fluxes in this latitude band, which is therefore accompanied also by large year-to-year variability of the mean fluxes. At 50°N, for example, the January-mean mean mass-flux, $[v][\sigma]$, in the layer between the isentropic levels at 300 K and 330 K varies between $-34\ \mathrm{kg\,m^{-1}K^{-1}s^{-1}}$ in 2007 and $+4\ \mathrm{kg\,m^{-1}K^{-1}s^{-1}}$ in 2010. The large equatorward mean mass-flux in January 2007 is mainly a response to the intense monthly-mean eddy PVS-flux in January 2007 ($6 \times 10^{-5}\ \mathrm{m\,s^{-2}}$). This implies that the *net* poleward mass-flux at 50°N is indirectly weakened by meridional eddy PVS-flux, as is verified in Fig. 8. Remembering that the *net* poleward mass-flux at 50°N is anti-correlated with the NAM-index at sea level (van Delden, 2024), it can be concluded that intense meridional eddy PVS-fluxes in the Middleworld will indirectly "drive" the NAM toward its positive phase. A sustained weakening of the eddy PVS-flux for some, as yet unknown, reason is needed to "drive" the NAM toward its negative phase, as we shall see in the next section.

The linear regression shown by the red line in Fig. 7 indicates that a weak Ferrel cell still exists (i.e. $[v][\sigma] < 0$) in the absence of eddy-forcing, i.e. when $[v^*\zeta^*] = 0$. This suggests that the Ferrel cell is not forced only by the *local* meridional eddy PVS-flux, but also probably by diabatic effects, such as radiative flux divergence, or by flow induced by distant changes to the PV-distribution, an important effect which is sometimes referred to as "action at a distance" (van Delden, 2024, section 5).

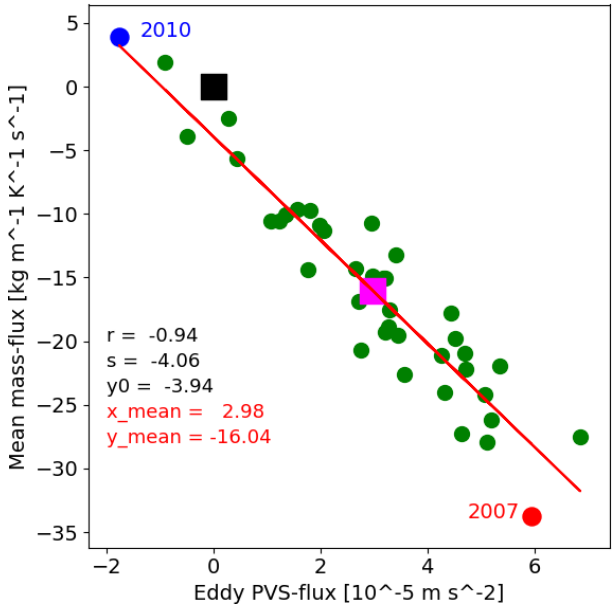

Figure 7. Showing that eddy PVS-flux drives the mean overturning circulation. The January-mean zonal-mean mean isentropic mass-flux, $[v][\sigma]$, in the layer between $\theta = 300$ K and $\theta = 330$ K at 50°N, as a function of the January-mean zonal-mean *eddy* PVS-flux, $[v^*\zeta^*]$, at $\theta = 315$ K at 50°N, in the years 1979-2018. The red straight line represents the best linear fit to the 40 points (correlation coefficient, $r = -0.94$). The black square is the origin. The magenta square represents the ensemble average value for all 40 months of January. The ensemble average eddy PVS-flux is $+2.98 \times 10^{-5}$ m s^{-2}. The ensemble average mean mass-flux is -14.26 kg m^{-1}K^{-1}s^{-1}. The blue dot is for January 2010 (extreme negative NAM-phase); the red dot is for January 2007 (extreme positive NAM-phase). Based on the ERA-Interim reanalysis (Dee et al., 2011).

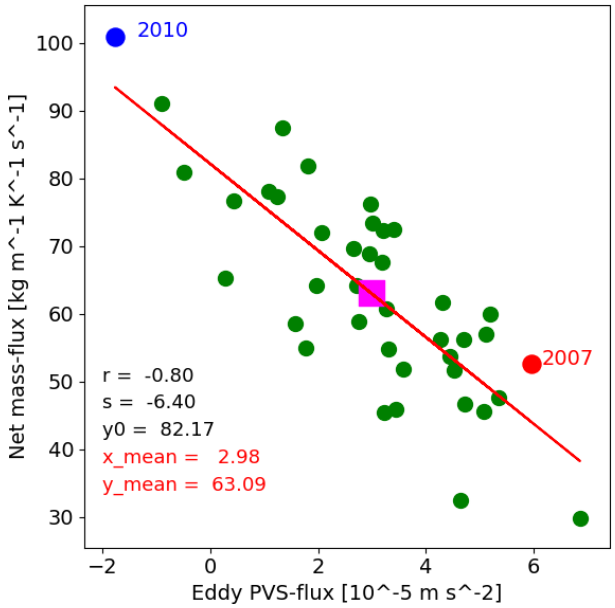

Figure 8. Showing that eddy PVS-flux reduces the net mass-flux (indirectly). The January-mean zonal-mean net isentropic meridional mass-flux, $[v\sigma]$, at 50°N in the layer between $\theta = 300$ K and $\theta = 330$ K as a function of the January-mean zonal-mean eddy isentropic meridional PVS-flux, $[v^*\zeta^*]$, at 315 K and 50°N, in the years 1979-2018. The red straight line represents the best linear fit to the 40 points (correlation coefficient, $r = -0.80$). The magenta square represents the ensemble average value for all 40 months of January. The ensemble average eddy PVS-flux is $+2.98 \times 10^{-5}$ m s^{-2}. The ensemble average net mass-flux is $+63.1$ kg m^{-1}K^{-1}s^{-1}. The blue dot is for January 2010 (extreme negative NAM-phase); the red dot is for January 2007 (extreme positive NAM-phase). Based on the ERA-Interim reanalysis (Dee et al., 2011).

7. A NAM-phase transition

Net meridional PVS-fluxes and accompanying intensity-changes of the circumpolar primary circulation in the Northern Hemisphere are relatively small on the monthly time-scale in January. That is why the January-mean circumpolar primary circulation is always close to thermal wind balance, which is why PV-inversion works on monthly average PV-fields (section 5 of van Delden, 2024). However, the exact manifestation of this balanced state, in terms of the intensity of the monthly mean circumpolar flow, such as the intensity of the STJ, is very different in different months of January. This is because the January-mean primary circulation is the result of averaging several different NAM-phase "events", which occurred in one month. This holds also for January 2007, as we shall see in the following. Evidence presented in the previous sections suggests that, because eddy PVS-fluxes are usually self-perpetuating in middle latitudes, the atmosphere in middle latitudes has a natural tendency to evolve toward the positive NAM-phase. Intense eddy PVS-fluxes, in turn, generate an intense secondary circulation, which counters the effect of eddies, specifically also in terms of mass-transfer. In other words, intense eddy PVS-fluxes are accompanied by weak net mass-fluxes, which helps the persistence of the positive NAM-phase, as happened during the first 18 days of January 2007.

After that date, however, a sustained decrease of the eddy PVS-flux in middle latitudes occurred, for some yet unknown reason. As expected, an abrupt and sustained increase of the net mass-flux occurred simultaneously, thereby forcing the NAM out of its positive polarity (Fig. 9).

Riviere and Drouard (2015) derive a composite negative NAM-*event*, defined as a period of time in which the NAM-index is at least one standard deviation below average. Based on a selection of 38 negative-NAM events, which meet this definition, they find that the composite negative NAM-event lasts 12 days. The negative-NAM event with

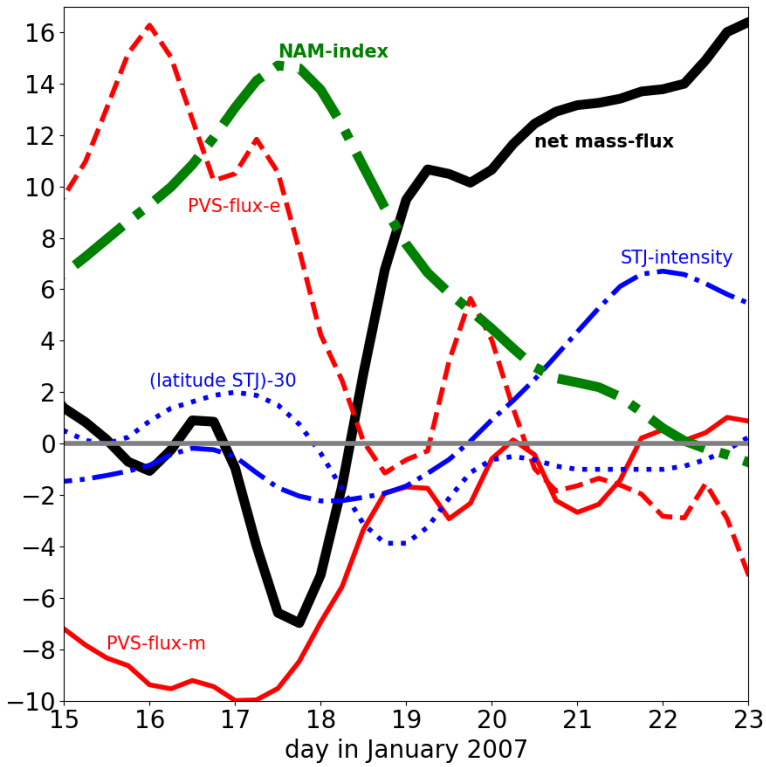

Figure 9. Anatomy of a positive to negative NAM-phase transition. Running daily means of the zonal-mean net isentropic meridional mass-flux, $[v\sigma]$, at 50°N in the layer between $\theta = 300$ K and $\theta = 330$ K in units of 10 kg s^{-1}m^{-1}K^{-1} (black thick solid curve), of the intensity of the Sub-Tropical Jet (STJ) (m s^{-1}) relative to the monthly average in January 2007 (42.8 m s^{-1}) (blue, dash-dotted), of the latitude of the STJ (°) relative to 30°N (blue, dotted), of the NAM-index (hPa) (green, thick dash-dotted), of the eddy PVS-flux, $[v^*\zeta^*]$ (10^{-5} m s^{-2}) at $\theta = 315$ K and 50°N (red, dashed) and of the mean PVS-flux, $[v][\zeta]$ (10^{-5} m s^{-2}) at $\theta = 315$ K and 50°N (red, solid) between 15 and 23 January 2007. Based on ERA-Interim reanalysis (Dee et al., 2011).

central date, 25 January 2007, is included in their set. The dimensional NAM-index is defined here simply as the zonal-mean sea level pressure difference between 35°N and 65°N relative to the 40-year daily January-climatology of the zonal-mean sea level pressure difference between 35°N and 65°N. The standard deviation of the daily running mean dimensional NAM-index in January is 5.1 hPa (based on 40 years of ERA-Interim data). With this definition of the NAM-index, the event centered around 25 January 2007 does not qualify as a negative NAM event. Nevertheless, the NAM-*transition* from extremely positive (3 standard deviations above normal) on 18 January 2007 to slightly negative on 22 January 2007 is interesting enough in itself to merit further investigation.

The steady decrease (i.e. at an approximately constant rate) of the NAM-index after 17 January (Fig. 9) indicates that this NAM-transition is due to the cumulative effect of sustained anomalously intense net poleward mass-fluxes. Within several days the middle latitude atmosphere is forced out of the feedback loop that very likely held it locked in its extreme positive NAM-phase until 18 January 2007. After this date, the eddy PVS-flux decreases from an average of nearly $+10^{-4}\,\mathrm{m\,s^{-2}}$ during the first 18 days of January 2007 to mainly negative values between 18 and 23 January 2007. Intense poleward mass transfer is also observed between these dates, coinciding with the steady decrease of the NAM-index from + 15 hPa to −1 hPa.

Consistent with expectations, the STJ-intensity, defined as the maximum value of $[u]$ in the Middleworld, increases by about $8\,\mathrm{m\,s^{-1}}$ between 18 and 22 January (Fig. 9), indicating an increase of the zonal-mean bulk baroclinicity at the poleward edge of the sub-tropics, presumably due to enhanced isentropic meridional mass-flux divergence just poleward of the STJ (Fig. 11 in van Delden, 2024).

What process initiates or forces this NAM-transition in January 2007? The Hovemöller diagram in Fig. 10 provides some hints. It shows the instantaneous meridional isentropic mass-flux, $v\sigma$, at 50°N in the layer between $\theta = 300$ K

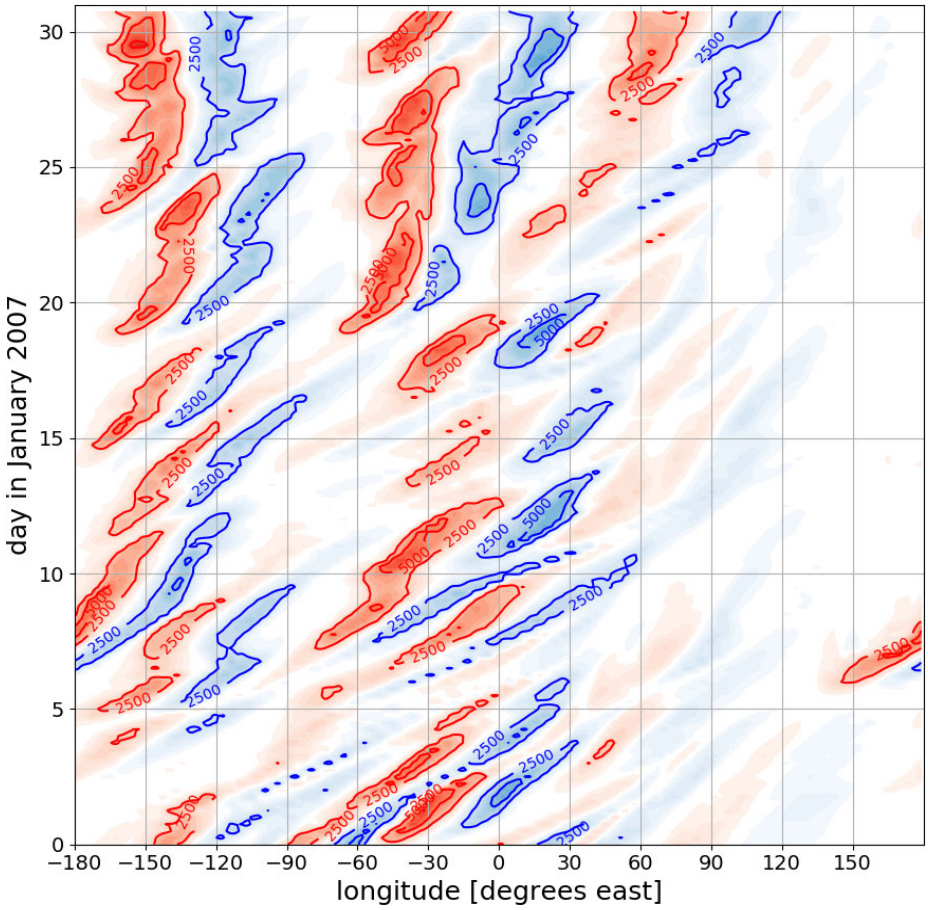

Figure 10. Showing that the NAM-transition is associated with a change of wave frequency and speed. Meridional component of the isentropic mass-flux at 50°N in the layer between between $\theta = 300$ K and $\theta = 330$ K as a function of time and longitude. Red (blue) shading corresponds to northward (southward) mass-flux. Absolute values of mass-fluxes are labeled in units of $\mathrm{kg\,s^{-1}m^{-1}K^{-1}}$. Based on the ERA-Interim reanalysis (Dee et al., 2011).

and $\theta = 330$ K as a function time and longitude in the month of January 2007. Alternating poleward and equatorward mass-flux pulses are observed, which last a few days between initial growth and final decay. These mass-flux pulses are associated with eastward travelling baroclinic planetary waves, which grow at preferred longitudes due to baroclinic instability, propagate eastward, and decay at different preferred longitudes. Wave amplitude-growth is manifest as an intensifying pulse of poleward mass-flux, indicated by red shading in Fig. 10. These *intensifying* poleward mass-flux pulses occur especially over the Central Pacific Ocean and the Western Atlantic Ocean. The eastward zonal phase speed of these pulses, which last about 3 to 6 days, appears to depend on the zonal wavelength of the wave. Before January 20th, the number of waves observed along a parallel is five to seven. January 20th marks a rather sudden transition to lower wave numbers (three to four) and to a much slower eastward wave propagation. The final amplitude-decay of the poleward mass-flux pulses is accompanied, with a certain time lag, by a pulse of equatorward mass-flux appearing to the east (downstream) of the original pulse of poleward mass-flux.

The wave-like features in the meridional isentropic mass-flux, seen in Fig. 10, are manifestations of planetary waves, travelling along the circumpolar wave-guide, formed by the mainly poleward potential vorticity gradient (Branstator, 2002). These planetary waves undergo baroclinic wave life cycles with life times of about 3 days before the transition on January 20th, while much longer life times are observed after this transition. For example, over the Pacific Ocean a baroclinic life cycle can be observed, starting on 11-12 January, with a poleward mass-flux pulse at 160°W. This feature travels eastward, reaching the longitude of 110°W, on 16 January. The poleward mass-flux pulse has bridged a distance of about 3500 km in about 4.5 days, implying a phase speed of 9 m s^{-1}. Between 5 and 10 January the eastward phase speed of the features in the meridional mass-flux over the Atlantic Ocean is much faster: approximately 15 m s^{-1}. Nevertheless, because $[u]$ at 50°N in the layer $\theta = 300$-330 K, in the first 18 days of January 2007, is in the order of 20 m s^{-1}, even the shortest waves propagate westward with respect to the mean flow.

Riviere and Drouard (2015) found that the sudden appearance of low-frequency anomalies in the middle latitude Pacific Ocean on 20 January 2007 is driven by anomalous intense convection in the tropical Pacific. Indeed, the "wave-regime transition" at 50°N on January 20th, in the layer between $\theta = 300$ K and $\theta = 330$ K, starts in the Central to East Pacific Ocean, and subsequently propagates eastwards, while weakening over North America, then propagating into the Atlantic and re-intensifying there (Fig. 10). After January 20th, pulses of poleward mass-flux exceed 5000 kg s^{-1} m^{-1} K^{-1} for many days at a fixed longitude, i.e. with negligible zonal displacement. The poleward mass-flux pulses usually exceed the equatorward mass-flux pulses in magnitude. This means that the net mass-flux is poleward, as is verified in Fig. 9.

As a final remark it is good to emphasize that a transition from one NAM-phase to the opposite NAM-phase is not abrupt. A NAM phase-transition is unlike the crossing of a tipping point in a non-linear mathematical system. Rather, a NAM phase-transition is the consequence of a relatively slow cumulative process associated with persistent anomalous meridional eddy fluxes of vorticity or anomalous net meridional fluxes of mass in middle latitudes. This idea was shown by Hinssen and Ambaum (2010) to apply also to the occurrence of Sudden Stratospheric Warmings (SSW's).

8. Conclusion

The old research question regarding the nature and cause of the Northern Annular Mode has until now been tackled by adopting pressure coordinates, assuming quasi-geostrophic balance and evaluating the effect of eddies on the zonal-mean state of the atmosphere in terms of meridional fluxes of momentum and heat, and so-called Eliassen-Palm fluxes. See, for example, the recent book by Wallace et al. (2023). By adopting isentropic coordinates and by not taking balance for granted, this and a companion paper offer a different perspective on the same research question. In isentropic coordinates, eddies affect the zonal-mean state of the atmosphere by means of meridional fluxes of vorticity and mass. The analysis in isentropic coordinates is simplified by the fact that isentropic surfaces are impermeable to vorticity-fluxes. Of course, problems arise when isentropic surfaces intersect the earth's surface. This happens by definition only in the Underworld (Fig. 2 of van Delden, 2024). Fortunately, the Underworld is rather sluggish compared to the Middleworld. In winter, the distribution of mass in the Underworld is determined principally by radiative cooling over cold surfaces and radiative heating over warm surfaces, which are relatively slow processes compared to the fast dynamics of cyclone live-cycles. driven mainly by intense baroclinicity in the Middleworld.

The Northern Annular Mode is identified here with the variability of the zonal-mean circumpolar circulation (the "primary circulation") in the Northern Hemisphere and its associated mass distribution. Northern Annular Mode variability is determined by interactions between the three fundamental components of the atmospheric general circulation in middle latitudes: (1) the primary circulation, (2) the zonal-mean meridional overturning circulation, called "secondary circulation", or Ferrel cell, and (3) the zonally asymmetric flow-component associated with large scale eddies, such as cyclones, anticyclones and planetary waves.

The primary circulation is usually in very close thermal wind balance. This implies that zonal-mean mass- and vorticity-distributions are coupled to each other in accordance with Kleinschmidt's principles, derived from PV-inversion, and enumerated in part 1 of this paper (van Delden, 2024). Eddies drive the primary circulation away from thermal wind balance by changing the zonal-mean mass- and vorticity-distributions in two essentially independent ways, i.e. by meridional advective eddy vorticity (PVS) fluxes and by meridional advective isentropic eddy mass-fluxes.

The atmosphere responds to eddy-induced thermal wind imbalances by creating a secondary circulation, which is again associated with meridional fluxes of both mass and PVS. PVS-fluxes due to the secondary circulation usually drive the primary circulation back to thermal wind balance. A robust manifestation of this response in the middle latitudes is the almost exact anti-correlation between the mean PVS-flux (due to the secondary circulation) and the eddy PVS-flux (Fig. 4). On a monthly time-scale, the secondary circulation in middle latitudes, in fact, practically nullifies the effect of eddies on the zonal-mean vorticity distribution. However, on a shorter time-scale, such as one day, the eddy PVS-flux exceeds the mean PVS-flux in absolute value if the eddy PVS-flux exceeds a positive threshold value, hence leading to intensification of the westerly flow associated with the primary circulation, otherwise leading to weakening of the primary circulation

The influence of net meridional PVS-fluxes on the primary circulation is easy to understand from the circulation theorem, which states that circulation around a circle of constant latitude, i.e. around a parallel, is proportional to the vorticity averaged over the area enclosed by that parallel. Eq. (15) is an expression of this connection between meridional PVS-fluxes and the rate of change of the intensity of the primary circulation. This paper shows that advective PVS-fluxes dominate the PVS-balance in January.

The largest PVS-flux variability is observed in the Middleworld in the latitude range between 50°N and 60°N. The extreme positive phase of the Northern Annular Mode (NAM) is characterized by intense poleward eddy PVS-fluxes in this latitude range, while the extreme negative NAM-phase is characterized by very weak eddy PVS-fluxes in this latitude range. Eddy PVS-fluxes in this latitude range are directed up the zonal-mean absolute vorticity gradient, which is poleward, principally because the meridional gradient of planetary vorticity is poleward (the β-effect). The NAM, therefore, is naturally inclined to evolve toward its positive phase. This might explain the skewed distribution of NAM-states. Positive NAM-state occur more frequently than negative NAM-states, but negative NAM-states are more extreme.

The negative NAM phase is characterized by relatively intense net poleward mass-fluxes in the Middelworld in middle latitudes. The associated mass-flux divergence maintains the intense baroclinicity at the poleward edge of the subtropics, which by thermal balance translates into an intense subtropical Jet (STJ). Baroclinicity supports the formation of planetary eddies, which push more mass poleward. This positive feedback loop, between zonal-mean baroclinicity and zonal-mean eddy mass-flux divergence, which promotes the negative NAM-phase, is presented in part 1 (van Delden, 2024) without going into the details of the separate roles of eddies and the secondary circulation. The present paper (part 2) adds the following important side-effect to this feedback loop. The intense STJ at 30°N, which is associated with the negative NAM-phase, is also associated on its poleward side with a strip of high relative vorticity, and further poleward, presumably between 45°N and 55°N, with a reduced poleward PVS-gradient. In view of Fig. 6, we then expect a relatively weak poleward eddy PVS-flux between 45°N and 55°N, and hence a weak secondary circulation in this latitude band, which is advantageous for the maintenance of the negative NAM-phase.

Acknowledgments. This paper is a follow-up of a workshop on the Northern Annular Mode held at IMAU (Utrecht University) on 19 April 2018. I thank the presenters (Maarten Ambaum, Frank Selten, Annalisa Cherchi, Wim Verkley, Wim van Caspel and Bob Ammerlaan) for their presentations and all participants for their contributions to discussions. Special thanks to Annalisa Cherchi for asking me, in the year 2019, to write a review paper about the NAM, and patiently encouraging me to come with this new perspective on the NAM.

List of symbols

c_p: specific heat at constant pressure ($c_p = 1004$ J kg^{-1}K^{-1})
f: Coriolis parameter or planetary vorticity ($f = 2\Omega \sin\phi$)
g: acceleration due to gravity ($g = 9.81$ m s^{-2})
$\vec{I}$: mass-flux vector (Eq. 7)
$\vec{J}$: vorticity (PVS) flux vector (Eq. 5)
p: pressure
p_{ref}: reference pressure (= 10^5 Pa)
T: temperature
u, v: zonal and merdional velocity
u_{gr}: gradient (balanced) wind
x, y, z: zonal, meridional and height coordinate
Z_θ: isentropic potential vorticity (Eq. 1)
ζ, ζ_a: relative vorticity, absolute vorticity ($\zeta_a = \zeta + f$)
θ: potential temperature (Eq. 1)
λ, ϕ: longitude, latitude,
σ: isentropic density (Eq. 3)
Ψ: isentropic streamfunction ($\Psi = c_pT + gz$)
Ω: earth's angular velocity ($\Omega = 7.3 \times 10^{-5}$ s^{-1})
Square brackets indicate a zonal mean, e.g. $[u] = \frac{1}{2\pi}\int_0^{2\pi} u d\lambda$

References

Ambaum, M. H. P. (1997). Isentropic formation of the tropopause, J. Atmos. Sci., 54, 555-568. doi:10.1175/1520-0469(1997)054<0555:IFOTT>2.0.CO;2.

Balasubramanian, G. and S. Garner (1997). The Role of Momentum Fluxes in Shaping the Life Cycle of a Baroclinic Wave, J. Atmos. Sci., 54, 510-533, doi:10.1175/1520-0469(1997)054<0510:TROMFI>2.0.CO;2.

Bennedict, J. J., S. Lee and S. B. Feldstein (2004). Synoptic view of the North Atlantic Oscillation, J. Atmos. Sci., 61, 121-144, doi:10.1175/1520-0469(2004)061<0121:SVOTNA>2.0.CO;2.

Birner, T., D. W. J. Thompson and T. G. Shepherd (2013). Up-gradient eddy fluxes of potential vorticity near the subtropical jet, Geophys. Res. Lett., 40, 5988-5993, doi:10.1002/2013GL057728.

Branstator, G. (2002). Circumglobal Teleconnections, the Jet Stream Waveguide and the North Atlantic Oscillation, J. Clim., 15, 1893-1910, doi:10.1175/1520 0442(2002)015<1893:CTTJSW>2.0.CO;2.

Butchart, N. (2014). The Brewer-Dobson circulation, Rev. Geophys., 52, 157-184, doi:10.1002/2013RG000448.

Charney, J. (1971). Geostrophic turbulence, J. Atmos. Sci., 28, 1088-1095, doi:10.1175/1520-0469(1971)028<1087:GT>2.0.CO;2.

Delden, A. J. van and Y. B. L. Hinssen (2012). PV-theta view of the zonal mean state of the atmosphere, Tellus, A, 64, 18710, doi:10.3402/tellusa.v64i0.18710.

Delden, A. J. van (2023). Physics of the Northern Annular Mode – Part 1: connection to meridional mass transfer, Ann. Geophys., doi:10.4401/ag-9013.

Dima, I. M. and J. M. Wallace (2003). On the seasonality of the Hadley cell, J. Atmos. Sci., 60, 1522-1527, doi:10.1175/1520-0469(2003)060<1522:OTSOTH>2.0.CO;2.

Dee, D. P., S. M. Uppala, A. J. Simmons, P. Berrisford et al. (2011). The ERA-Interim reanalysis: configuration and performance of the data assimilation system, Quart. J. R. Met. Soc., 137, 553-597, doi:10.1002/qj.828.

Dutton, J. A. (1976). The Ceaseless Wind, Dover Publications, 617, ISBN: 0-486-65096-0.

Eliassen, A. (1951). Slow thermally or frictionally controlled meridional circulation in a circular vortex, Astrophysica Norvegica, 5, 19-60.

Haynes, P. H. and M. E. McIntyre (1990). On the conservation and impermeability theorems for potential vorticity, J. Atmos. Sci., 47, 2021-2031, doi:10.1175/1520-0469(1990)047<2021:OTCAIT>2.0.CO;2.

Hinssen, Y. B. L. and M. P. H. Ambaum, (2010). Relation between the 100 hPa heat flux and stratospheric potential vorticity, J. Atmos. Sci., 67, 4027-4027, doi:10.1175/2010JAS3569.1.

Kuo, H. L. (1951). Vorticity transfer as related to the development of the general circulation, J. Atmos. Sci., 8, 307-315, doi:10.1175/1520-0469(1951)008<0307:VTARTT>2.0.CO;2.

Hoskins, B. J., M. E. McIntyre and A. W. Robertson (1985). On the use and significance of isentropic potential vorticity maps, Quart. J. R. Met. Soc., 111, 877-946, doi:10.1002/qj.49711147002.

Kuo, H. L. (1956). Forced and free meridional circulations in the atmosphere, J. Atmos. Sci., 13, 561-568, doi:10.1175/1520-0469(1956)013<0561:FAFMCI>2.0.CO;2.

Li, J. and J. X. L. Wang (2003). A modified zonal index and its physical sense, Geophys. Res. Lett., 30, 1632, doi:10.1029/2003GL017441.

McIntyre, M. E. (1982). How well do we understand the dynamics of stratospheric warmings?, J. Meteorol. Soc. Japan, 60, 37-65, doi:10.2151/jmsj1965.60.1_37.

Plumb, R. A. and J. Eluszkiewicz (1999). The Brewer-Dobson circulation: Dynamics of tropical upwelling, J. Atmos. Sci., 56, 868-890, doi:10.1175/1520-0469(1999)056<0868:TBDCDO>2.0.CO;2.

Riviere, G. and M. Drouard (2015). Dynamics of the Northern Annular Mode at Weekly Time Scales, J. Atmos. Sci., 72, 4569-4590, doi:10.1175/JAS-D-15-0069.1.

Starr, V. P. (1948). An essay on the general circulation of the earth's atmosphere, J. Atmos. Sci., 5, 39-43, doi:10.1175/1520-0469(1948)005<0039:AEOTGC>2.0.CO;2.

Starr, V. P. (1968). Physics of Negative Viscosity Phenomena, MacGraw-Hill, 256, ISBN:978-00700608757.

Thorncroft, C. D., B. J. Hoskins and M. E. McIntyre (1993). Two paradigms of baroclinic-wave life-cycle behaviour, Q. J. R. Meteorol. Soc., 119, 17-55, doi:10.1002/qj.49711950903.

Wallace, J. M., D. S. Battisti, D. W. J. Thompson and D. L. Hartmann (2023). The Atmospheric General Circulation, Cambridge University Press, 406, ISBN:978-1-108-47424-5.

***CORRESPONDING AUTHOR: Aarnout J. VAN DELDEN**,
Institute for Marine and Atmospheric Research Utrecht (IMAU), Physics Department, Utrecht University,
Princetonplein 5, 3584CC Utrecht, the Netherlands
e-mail: a.j.vandelden@uu.nl